Acta Crystallographica Section F
**Structural Biology and Crystallization Communications**
ISSN 1744-3091

# Expression, crystallization and preliminary X-ray crystallographic analysis of human agmatinase

**Kyoung Hoon Kim, Hyung Jun Ahn, Do Jin Kim, Hyung Ho Lee, Jun-Yong Ha, Hye-Kyung Kim, Hye-Jin Yoon and Se Won Suh***

Department of Chemistry, College of Natural Sciences, Seoul National University, Seoul 151-742, South Korea

Correspondence e-mail: sewonsuh@snu.ac.kr

Received 9 August 2005
Accepted 28 August 2005
Online 13 September 2005

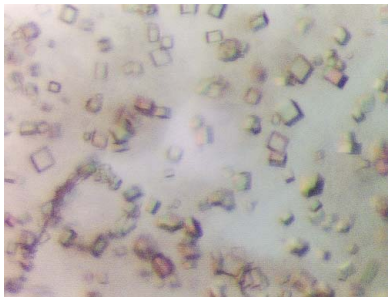



Agmatine, which results from the decarboxylation of L-arginine by arginine decarboxylase, is a metabolic intermediate in the biosynthesis of putresine and higher polyamines (spermidine and spermine). Recent studies indicate that agmatine can have several important biochemical effects in humans, ranging from effects on the central nervous system to cell proliferation in cancer and viral replication. Agmatinase catalyses the hydrolysis of agmatine to putresine and urea and is a major target for drug action and development. The human agmatinase gene encodes a 352-residue protein with a putative mitochondrial targeting sequence at the N-terminus. Human agmatinase (residues Ala36–Val352) has been overexpressed as a fusion with both N- and C-terminal purification tags in *Escherichia coli* and crystallized in the presence of $Mn^{2+}$ and 1,6-diaminohexane at 297 K using polyethylene glycol 4000 as a precipitant. X-ray diffraction data were collected at 100 K to 2.49 Å from a flash-frozen crystal. The crystals are tetragonal, belonging to space group $P4_2$, with unit-cell parameters $a = b = 114.54$, $c = 125.65$ Å, $\alpha = \beta = \gamma = 90^\circ$. Three monomers are likely to be present in the asymmetric unit, giving a crystal volume per protein weight ($V_M$) of 3.66 Å$^3$ Da$^{-1}$ and a solvent content of 66.4%.

## 1. Introduction

Putrescine, spermidine and spermine are the main polyamines found in prokaryotes and eukaryotes. The diamine putrescine is the precursor used in biosynthesis of spermidine and spermine. In the classical pathway for polyamine biosynthesis, putrescine is formed from L-arginine in two steps by the consecutive actions of arginase and ornithine decarboxylase (ODC). Arginase removes urea from the terminal guanidine moiety of L-arginine to produce ornithine and the resulting ornithine is decarboxylated to putrescine by ODC. An alternative pathway for polyamine biosynthesis has also been described in which arginine is first decarboxylated to agmatine (1-amino-4-guanidinobutane) by arginine decarboxylase (ADC) followed by removal of urea to form putrescine by agmatinase (agmatine ureohydrolase; EC 3.5.3.11). Until the mid-1990s, ADC and agmatinase were not believed to be expressed in mammals. However, in 1994 agmatine was identified as an endogenous ligand for the imidazoline receptor (Li *et al.*, 1994), and ADC and agmatinase were subsequently identified in mammalian brain (Reis & Regunathan, 1998; Sastre *et al.*, 1996). Several lines of evidence indicate that agmatinase may play important roles in mammals including the regulation of neurotransmitter-related functions (Reis & Regunathan, 1998, 2000).

Polyamines affect numerous processes in carcinogenesis and the association of increased polyamine synthesis with cell growth and cancer has been known for many years (Gerner & Meyskens, 2004). Increased polyamine levels are associated with increased cell proliferation, decreased apoptosis and increased expression of genes affecting tumour invasion and metastasis. Polyamines are also necessary for angiogenesis occurring in response to tumour growth. Conversely, suppression of polyamine levels is associated with decreased cell growth, increased apoptosis and decreased expression of genes affecting tumour invasion and metastasis (Gerner & Meyskens, 2004). Difluoromethylornithine (DFMO), which irreversibly inactivates ODC, is the most widely studied example of a

polyamine-metabolism inhibitor that suppresses cancer development in animal models (Meyskens & Gerner, 1999). Although DFMO is a potent inhibitor of carcinogenesis in animal models, DFMO either alone or in combination with other chemotherapies was generally found to have little antitumour activity in clinical trials (Gerner & Meyskens, 2004).

However, combinations of DFMO and non-steroidal anti-inflammatory drugs were shown to be potent in chemoprevention in experimental models (Gerner & Meyskens, 2004). Interventions at several points in polyamine metabolism might be necessary to optimally repress the development of epithelial cancers. One possibility is the inhibition of agmatinase activity. The importance of putrescine biosynthesis by the ADC-agmatinase pathway in the growth of some cancers is supported by the analysis of Iyer *et al.* (2002). This suggests that agmatinase activity might be advantageous for tumour growth. By regulating the levels of its bioactive substrate, agmatinase is likely to have a significant influence on the functions of a variety of organ systems and may facilitate tumour growth and increase the severity of a primary neuronal injury. Specific inhibitors of agmatinase may be useful for the treatment of some types of cancer, as well as in reducing the extent of neuronal injury and alleviating morphine dependence (Iyer *et al.*, 2002). Agmatinase expression was found to be elevated upon hepatitis B virus infection and may provide a source of polyamines for efficient viral replication. If so, inhibition of hepatic agmatinase activity could represent a new treatment strategy for patients with viral hepatitis (Mistry *et al.*, 2002).

The amino-acid sequences of agmatinases indicate their homology to arginases, suggesting a common evolutionary origin (Sekowska *et al.*, 2000; Ouzounis & Kyrpides, 1994; Perozich *et al.*, 1998). The human agmatinase gene encodes a 352-residue protein with a putative mitochondrial targeting sequence at the amino-terminus (Iyer *et al.*, 2002; Mistry *et al.*, 2002). The cleavage site was predicted to exist between Gln35 and Ala36 (Dallmann *et al.*, 2004). Human mitochondrial agmatinase has 35% sequence identity to *Escherichia coli* agmatinase, and 20 and 24% identity to human arginases I and II (Iyer *et al.*, 2002), respectively. The residues required for binding of $Mn^{2+}$ at the active site in bacterial agmatinases and other members of the arginase superfamily are fully conserved in human agmatinase (Mistry *et al.*, 2002; Iyer *et al.*, 2002).

While a wealth of structural data is available on arginases, structural analysis of agmatinases is limited to our previous work on *Deinococcus radiodurans* agmatinase (Lee *et al.*, 2004; Ahn *et al.*, 2004). This showed that *D. radiodurans* agmatinase exists as a compact homohexamer of 32 symmetry and its binuclear manganese cluster is highly similar but not identical to those of arginase and proclavaminate amidinohydrolase. In order to provide a structural basis for better understanding the functional roles of agmatinase in vertebrates, including humans, and for the discovery of inhibitors, determination of the three-dimensional structure of mammalian agmatinases is necessary. In this study, we have overexpressed human agmatinase (residues Ala36–Val352) fused with both N- and C-terminal purification tags in *E. coli* and crystallized it. We report here its crystallization conditions and preliminary X-ray crystallographic data.

## 2. Experimental

### 2.1. Protein expression and purification

The gene encoding human agmatinase (residues Ala36–Val352) was amplified by polymerase chain reaction using the human kidney cDNA library as template. The forward and reverse oligonucleotide primers designed using the published gene sequence (SWISS-PROT; http://www.expasy.ch/) were 5′-G GAA TTC **CAT ATG** GCT TCC GAC GCG CCC CGG-3′ and 5′-CCG CCG **CTC GAG** GAC GGT TGT CAC TTT GGG GAG AG-3′, respectively, where the bases in bold represent the *Nde*I and *Xho*I restriction-enzyme cleavage sites. The amplified DNA was inserted into the *Nde*I/*Xho*I-digested expression vector pET-28b(+) (Novagen). This vector construction adds an eight-residue tag (LEHHHHHH) to the carboxy-terminus and a 20-residue tag (MGSSHHHHHHSSGLVPRGSH) in front of the amino-terminal methionine of the recombinant agmatinase to facilitate purification. The protein was overexpressed in *E. coli* BL21-CodonPlus(DE3)-RIL cells (Stratagene). Cells were grown at 310 K to an $OD_{600}$ of 0.5 in Terrific Broth medium containing 50 µg ml$^{-1}$ kanamycin and protein expression was induced by 1.0 m*M* isopropyl *β*-D-thiogalactopyranoside (IPTG). Cells growth continued at 293 K for 18 h after IPTG induction and cells were harvested by centrifugation at 4200*g* (6000 rev min$^{-1}$; Sorvall GSA rotor) for 10 min at 277 K. The cell pellet was resuspended in ice-cold lysis buffer (20 m*M* Tris–HCl pH 7.9, 500 m*M* sodium chloride, 5 m*M* imidazole and 1 m*M* phenylmethylsulfonyl fluoride) and was then homogenized using an ultrasonic processor. The crude lysate was centrifuged at 70 400*g* (30 000 rev min$^{-1}$; Beckman 45Ti rotor) for 1 h at 277 K and the recombinant protein in the supernatant fraction was purified in two chromatographic steps. The first step utilized the hexahistidine tags by metal-chelate chromatography on Ni–NTA resin (Qiagen). Gel filtration was then performed on a HiLoad XK 16 Superdex 200 prep-grade column (Amersham-Pharmacia) which was previously equilibrated with buffer *A* (50 m*M* Tris–HCl pH 7.5, 100 m*M* sodium chloride and 1 m*M* manganese sulfate). The homogeneity of the purified protein was assessed by SDS–PAGE (Laemmli, 1970). The protein solution was concentrated using an YM10 ultrafiltration membrane (Amicon). The protein concentration was estimated by measuring the absorbance at 280 nm, employing the calculated extinction coefficient of 17 210 $M^{-1}$ cm$^{-1}$ (SWISS-PROT; http://www.expasy.ch/).

### 2.2. Crystallization

Crystallization was performed at 297 K by the hanging-drop vapour-diffusion method using 24-well tissue-culture plates. Each hanging drop was prepared by mixing equal volumes (3 µl each) of protein solution (0.45 m*M* monomer concentration dissolved in buffer *A*) and reservoir solution, followed by addition of the inhibitor solution (0.3 µl 360 m*M* 1,6-diaminohexane in buffer *A*). This results in an approximately 1:40 molar ratio of agmatinase monomer to inhibitor and 0.5 m*M* $Mn^{2+}$ ions. Each hanging drop on a siliconized cover slip was placed over 0.48 ml reservoir solution. Initial crystallization conditions were established using screening kits from Hampton Research (Crystal Screens I and II and MembFac) and from deCODE Biostructures Group (Wizard I and II).

### 2.3. X-ray diffraction experiment

Crystals were flash-frozen using a cryoprotectant solution consisting of 0.2 *M* ammonium acetate, 0.1 *M* trisodium citrate pH 5.6, 30%(*w*/*v*) polyethylene glycol 4000 and 30%(*v*/*v*) glycerol. Crystals were soaked in 5 µl cryoprotectant solution for 10 s before being flash-frozen in liquid nitrogen. X-ray diffraction data were collected at 100 K using an Area Detector System Corporation Quantum 210 CCD detector at the experimental station NW12A of Photon Factory, Japan. The crystal was rotated through a total of 180° with a 1.0° oscillation range per frame. The wavelength of the synchrotron radiation was 1.2028 Å. The raw data were processed

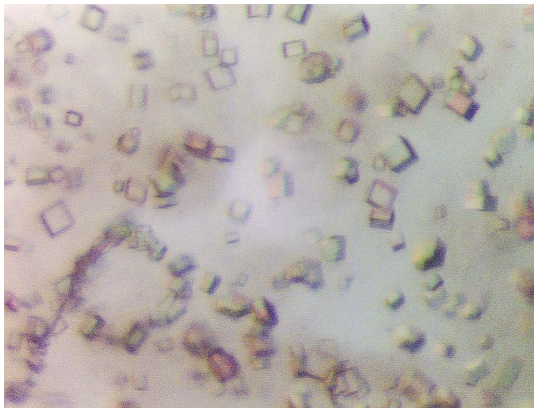

**Figure 1**
Crystals of human agmatinase. The largest crystals have approximate dimensions of 0.2 × 0.2 × 0.2 mm.

and scaled using the *HKL*2000 program package (Otwinowski & Minor, 1997).

## 3. Results and discussion

When we tried to express full-length human agmatinase in *E. coli*, fused either with an N-terminal 20-residue tag (MGSSHHHH-HHSSGLVPRGSH) alone or with both the N-terminal tag and a C-terminal eight-residue tag (LEHHHHHH), the protein was not expressed. When we expressed the construct spanning residues Glu48–Val352 of human agmatinase with both the N- and C-terminal tags in *E. coli* BL21-CodonPlus(DE3)-RIL cells, the protein was expressed at a very low level (∼1 mg purified enzyme per litre of culture). When we expressed the Ala36–Val352 construct with both the N- and C-terminal tags, it was expressed in a soluble form with a much higher yield of ∼5 mg purified enzyme per litre of culture. Without the C-terminal tag, the expression level was considerably lower. Therefore, we chose to crystallize the human agmatinase Ala36–Val352 fused with both the N- and C-terminal tags.

The presence of both N- and C-terminal tags did not prevent the recombinant enzyme from forming crystals that are suitable for structure determination at sufficiently high resolution. We obtained the best crystals using a reservoir solution comprised of 0.2 *M* ammonium acetate, 0.1 *M* trisodium citrate pH 5.6, 30%(*w*/*v*) polyethylene glycol 4000. Isometric crystals grew to approximate dimensions of 0.2 × 0.2 × 0.2 mm within 2 d (Fig. 1). A set of diffraction data was collected to 2.49 Å from a flash-frozen crystal. Table 1 summarizes the statistics of data collection. The space group was determined to be $P4_2$ on the basis of systematic absences and the unit-cell parameters are $a$ = 114.54, $b$ = 114.54, $c$ = 125.65 Å, $\alpha = \beta = \gamma = 90^\circ$. If we assume that three monomers are present in the crystallographic asymmetric unit, the crystal volume per protein weight ($V_M$) is 3.66 Å$^3$ Da$^{-1}$ (Matthews, 1968) and the solvent content is 66.4%.

Proclavaminate amidinohydrolase from *Streptomyces clavuligerus* and agmatinase from *D. radiodurans* show 39 and 36% sequence identity to Ser46–Leu343 and Gly55–Cys344 of human agmatinase, respectively. However, we could not solve the structure of human agmatinase by molecular replacement using these enzymes as models (Elkins *et al.*, 2002; Ahn *et al.*, 2004). Of the members of the mammalian ureohydrolase superfamily, crystal structures are available for rat liver arginase I (Kanyo *et al.*, 1996) and human extrahepatic arginase II (Cama *et al.*, 2003). They show 25 and 27% identity to human agmatinase (Ile76—Pro323 and Ala74—Ala345), respectively. Molecular-replacement trials with these structures also failed to give a solution. We plan to solve the structure by other methods such as multiwavelength anomalous diffraction.

**Table 1**
Data-collection statistics.

Values in parentheses refer to the highest resolution shell (2.58–2.49 Å).

| | |
|---|---|
| X-ray wavelength (Å) | 1.2028 |
| Temperature (K) | 100 |
| Space group | $P4_2$ |
| Unit-cell parameters (Å) | $a = b$ = 114.54, $c$ = 125.65 |
| Resolution range (Å) | 50–2.49 |
| Total/unique reflections | 1082519/56560 |
| $R_{merge}$† (%) | 9.5 (41.9) |
| Data completeness (%) | 100 (100) |
| Average $I/\sigma(I)$ | 30.6 (5.1) |

† $R_{merge} = \sum_h \sum_i |I(h)_i - \langle I(h)\rangle| / \sum_h \sum_i I(h)_i$, where $I(h)_i$ is the intensity of the $i$th measurement of reflection $h$ and $\langle I(h)\rangle$ is the mean value of $I(h)$ for all $i$ measurements.

We thank the staff at beamline NW12A of Photon Factory, Japan for assistance during data collection. This work was supported by the Center for Functional Analysis of Human Genome (21st Century Frontier Program of the Korea Ministry of Science and Technology). KHK, HJA, DJK, HHL and JYH are supported by BK21 Fellowships. KHK is supported by the Seoul Science Fellowship.

## References

Ahn, H. J., Kim, K.-H., Lee, J., Ha, J.-Y., Lee, H. H., Kim, D., Yoon, H.-J., Kwon, A. R. & Suh, S. W. (2004). *J. Biol. Chem.* **279**, 50505–50513.
Cama, E., Colleluori, D. M., Emig, F. A., Shin, H., Kim, S. W., Kim, N. N., Traish, A. M., Ash, D. E. & Christianson, D. W. (2003). *Biochemistry*, **42**, 8445–8451.
Dallmann, K., Junker, H., Balabanov, S., Zimmermann, U., Giebel, J. & Walther, R. (2004). *Int. J. Cancer*, **108**, 342–347.
Elkins, J. M., Clifton, I. J., Hernandez, H., Doan, L. X., Robinson, C. V., Schofield, C. J. & Hewitson, K. S. (2002). *Biochem. J.* **366**, 423–434.
Gerner, E. W. & Meyskens, F. L. Jr (2004). *Nature Rev. Cancer*, **4**, 781–792.
Iyer, R. K., Kim, H. K., Tsoa, R. W., Grody, W. W. & Cederbaum, S. D. (2002). *Mol. Genet. Metab.* **75**, 209–218.
Kanyo, Z. F., Scolnick, L. R., Ash, D. E. & Chistianson, D. W. (1996). *Nature (London)*, **383**, 554–557.
Laemmli, U. K. (1970). *Nature (London)*, **227**, 680–685.
Lee, J. A., Ahn, H. J., Ha, J.-Y., Shim, S. M., Kim, K.-H., Kim, H. K. & Suh, S. W. (2004). *Acta Cryst.* D**60**, 1890–1892.
Li, G., Regunathan, S., Barrow, C. J., Eshraghi, J., Cooper, R. & Reis, D. J. (1994). *Science*, **263**, 966–969.
Matthews, B. W. (1968). *J. Mol. Biol.* **33**, 491–493.
Meyskens, F. L. Jr & Gerner, E. W. (1999). *Clin. Cancer Res.* **5**, 945–951.
Mistry, S. K., Burwell, T. J., Chambers, R. M., Rudolph-Owen, L., Spaltmann, F., Cook, W. J. & Morris, S. M. Jr (2002). *Am. J. Physiol. Gastrointest. Liver Physiol.* **282**, G375–G381.
Otwinowski, Z. & Minor, W. (1997). *Methods Enzymol.* **276**, 307–326.
Ouzounis, C. A. & Kyrpides, N. C. (1994). *J. Mol. Evol.* **39**, 101–104.
Perozich, J., Hempel, J. & Morris, S. M. Jr (1998). *Biochem. Biophys. Acta*, **1382**, 23–37.
Reis, D. J. & Regunathan, S. (1998). *J. Auton. Nerv. Syst.* **72**, 80–85.
Reis, D. J. & Regunathan, S. (2000). *Trends Pharmacol. Sci.* **21**, 187–193.
Sastre, M., Regunathan, S., Galea, E. & Reis, D. J. (1996). *J. Neurochem.* **67**, 1761–1765.
Sekowska, A., Danchin, A. & Risler, J. L. (2000). *Microbiology*, **146**, 1815–1828.